

## A review on UV/TiO<sub>2</sub> photocatalytic oxidation process

Ramesh Thiruvengatchari, Saravanamuthu Vigneswaran<sup>†</sup> and Il Shik Moon\*

Faculty of Engineering, University of Technology, Sydney, P.O. Box 123, Broadway, NSW 2007, Australia

\*Faculty of Engineering, Suncheon National University, 315 Maegok Dong, Suncheon, Chonnam 540-742, Korea

(Received 24 July 2006 • accepted 29 May 2007)

**Abstract**—Advanced oxidation processes (AOPs) with UV irradiation and photocatalyst titanium dioxide (TiO<sub>2</sub>) are gaining growing acceptance as an effective wastewater treatment method. A comprehensive review of the UV-TiO<sub>2</sub> photocatalytic oxidation process was conducted with an insight into the mechanism involved, catalyst TiO<sub>2</sub>, irradiation sources, types of reactors, comparison between effective modes of TiO<sub>2</sub> application as immobilized on surface or as suspension, and photocatalytic hybrid membrane system. Photocatalytic degradation technique with titanium dioxide is generally applied for treating wastewater containing organic contaminants due to its ability to achieve complete mineralization of the organic contaminants under mild conditions such as ambient temperature and ambient pressure. Recently, photocatalysis studies using TiO<sub>2</sub> have been gaining attention for the degradation of persistent organic pollutants and other organic chemicals which are known to be endocrine disruptors. Treatment of wastewater in a titanium dioxide-suspended slurry reactor has been widely utilized due to its simplicity and enhanced degradation efficiency. However, this system requires separation of TiO<sub>2</sub> from water after the photocatalytic process. The final section of the manuscript focuses on the removal of TiO<sub>2</sub> using a membrane hybrid system. A two-stage coagulation and sedimentation process coupled with microfiltration hollow-fibre membrane process was found to achieve complete removal of TiO<sub>2</sub>, and the recovered TiO<sub>2</sub> can be reused for a photocatalytic process after regeneration.

Key words: Photocatalytic Oxidation, TiO<sub>2</sub>, UV Light, Solar Energy, Membrane, Hybrid System

### INTRODUCTION

Advanced oxidation processes (AOP), which involve the generation of highly reactive hydroxyl radical (HO·), have emerged as a promising water and wastewater treatment technology for the degradation or mineralization of a wide range of organic contaminants. A class of AOP consists of photoactivated processes. The photoactivated reactions are characterized by the free radical mechanism initiated by the interaction of photons of a proper energy level with the catalyst (photocatalytic oxidation). The present review aims to provide a comprehensive analysis on the mechanism of UV-TiO<sub>2</sub> photocatalytic oxidation process, photocatalyst material, irradiation sources and the types of photoreactors. The efficiency of the system is also affected by the mode of TiO<sub>2</sub> application as immobilized on surface or as suspension.

TiO<sub>2</sub> photocatalysis is effective for the decomposition of various organic contaminants in water; however, its practical use as slurry type suspensions is limited because of the difficulty of separation of the infinitesimally small TiO<sub>2</sub> particles after the photocatalytic process. This final section of the manuscript provides a specific insight into the separation of TiO<sub>2</sub> from suspension by a photocatalytic hybrid membrane system.

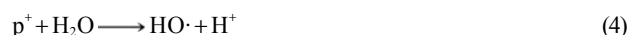
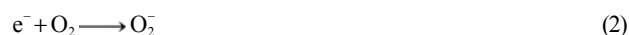
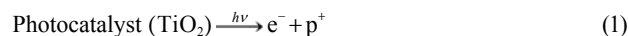
#### 1. Photocatalytic Oxidation

Although Frank and Bard [1] were the first to examine the possibility of using a semiconductor catalyst (titanium dioxide-TiO<sub>2</sub>) to decompose cyanide, Ollis and co-workers extensively studied the potential of photocatalysis for organic degradation [2-5].

Semiconductors are primary light absorbers. They are used in

photocatalysis because of a favorable combination of electronic structure, light absorption properties, charge transport characteristics, and excited-state lifetimes [6]. The principal mechanism of a semiconductor photocatalytic reaction (Fig. 1) is as follows. When a photocatalytic surface is illuminated by light with energy equal to or larger than the bandgap energy  $\Delta E_{bg}$  (bandgap energies of common semiconductors are given in Table 1), it excites the electrons in the valance band to the conduction band, resulting in the formation of a positive hole ( $p^+$ ) in the valance band and an electron ( $e^-$ ) in the conduction band.

The positive hole oxidizes either pollutants directly or water to produce HO· radicals, whereas the electron in the conduction band reduces oxygen adsorbed to photocatalyst (TiO<sub>2</sub>). The mechanism described above can be represented by Eqs. (1)-(5) as shown below;



In the photocatalytic degradation of the pollutants, when the reduction process of oxygen (Eq. (2)) and the oxidation of pollutants (Eq. (3) and (4)) do not proceed simultaneously, there is an electron accumulation in the conduction band, thereby causing a recombination of electron and positive holes. Therefore, efficient consumption of electrons is essential to promote photocatalytic oxidation.

The most important and fundamental elements for a successful photocatalytic system are the catalyst, the light source and the reactor configuration.

<sup>†</sup>To whom correspondence should be addressed.

E-mail: S.vigneswaran@uts.edu.au

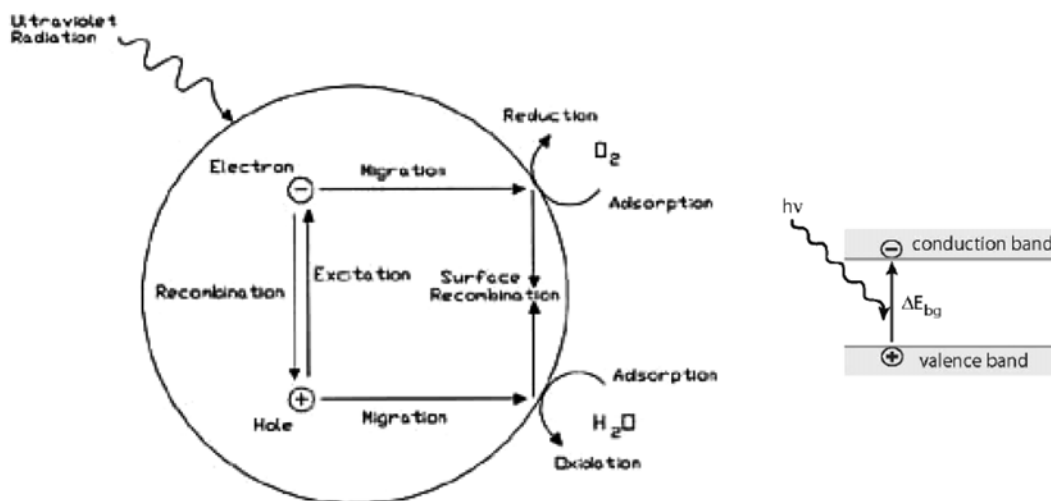


Fig. 1. Schematic representation of the mechanism of photocatalytic activity (photochemical activation and electron-hole formation) [7].

Table 1. Bandgap energies for some common semiconductor materials at 0 K [8-10]

Semiconductors	Bandgap energy (eV)	Semiconductors	Bandgap energy (eV)
Diamond	5.4	WO <sub>3</sub>	2.76
CdS	2.42	Si	1.17
ZnS	3.6	Ge	0.744
ZnO	3.436	Fe <sub>2</sub> O <sub>3</sub>	2.3
TiO <sub>2</sub>	3.03	PbS	0.286
CdS	2.582	PbSe	0.165
SnO <sub>2</sub>	3.54	ZrO <sub>2</sub>	3.87
CdSe	1.7	Cu <sub>2</sub> O	2.172

## 2. TiO<sub>2</sub> as Catalyst

Among many semiconductor photocatalysts, there is a general consensus among researchers that TiO<sub>2</sub> is more superior because of its high activity, large stability to light illumination, low price, and nontoxicity [6,10-16]. Okomoto [11,12] observed the greater photocatalytic activity for TiO<sub>2</sub> compared to CdS catalyst for the decomposition of phenol as target organic species. Sakthivel [10] showed that under similar study conditions, TiO<sub>2</sub> had greater photocatalytic efficiency than  $\alpha$ -Fe<sub>2</sub>O<sub>3</sub>, ZrO<sub>2</sub>, CdS, WO<sub>3</sub> and SnO<sub>2</sub>. However, ZnO performed better than TiO<sub>2</sub>. However, Augugliaro [13] indicated that, although ZnO had a higher activity (although the surface area is less) than TiO<sub>2</sub>, the later was photochemically more stable in aqueous media. Wu [17] also observed higher photocatalytic activity for TiO<sub>2</sub> compared to ZnO and SnO<sub>2</sub>.

Significant progress has been made on investigating the photocatalytic activity of TiO<sub>2</sub> based on its crystal structure and size [15, 18]. Three different crystal forms exist: anatase, rutile and brookite. Anatase and rutile have been the most studied phases of nanostructured TiO<sub>2</sub>, while reports on brookite are still scarce [6,13,18-22]. The position of oxygen ions on the exposed crystal surface of anatase shows a triangular arrangement, allowing effective absorption of organics. Whereas, the position of titanium ions creates a favorable reaction condition with the absorbed organics. However, this

favorable structure arrangement is not available for rutile structure. This is one of the reasons why anatase has higher photocatalytic activity than rutile [23,24]. The difference in abilities is also reported to be due to their electronic and chemical properties [13]. Even though anatase is believed to be the most active form of titania, reports suggest that a pure anatase sample would not necessarily lead to the best photocatalytic performance [25-27]. The presence of rutile phase introduces mesoporosity and a wider pore size distribution. These factors may be responsible for the increased catalytic activity. These reports suggest that a mixture of anatase and rutile would be the best combination to achieve maximum photocatalytic efficiency. Several commercial samples of TiO<sub>2</sub> varying in particle size and purity were studied to determine catalytic activity with Degussa P25 grade (mixture of 70% anatase, 30% rutile material). There is a general consensus that Degussa P-25 TiO<sub>2</sub> gives better degradation efficiency compared to other forms [10,26,28].

The effect of particle size on the photocatalytic activity can be interpreted in terms of surface area (anatase=10 m<sup>2</sup>/g, rutile=20 m<sup>2</sup>/g, Degussa P25=50 m<sup>2</sup>/g). Generally, the smaller the particle size, the larger the surface area and higher the expected activity. This can be explained in terms of an increase in number of active sites per square meter, as well as greater adsorbability of the pollutants on the catalyst surface [29].

## 3. Light Source

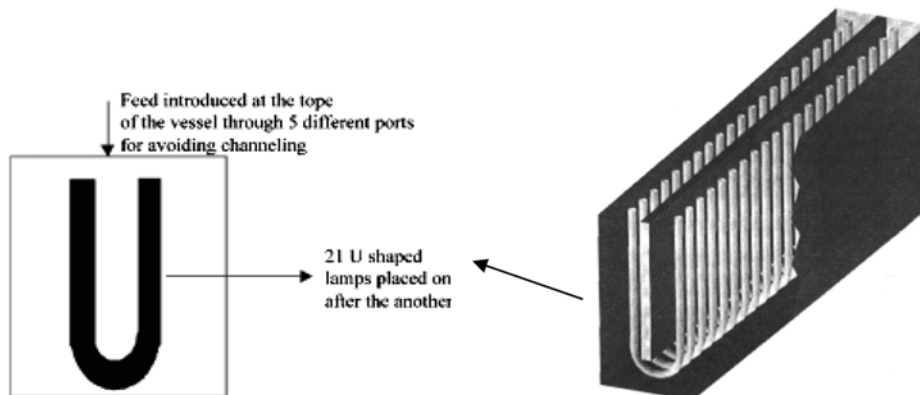
TiO<sub>2</sub> absorbs radiation below the visible range of light spectrum. Hence, photoactivation of TiO<sub>2</sub> requires radiation with light of wavelength less than or equal to 384 nm, with an absorbance maximum at approximately 340 nm. The vast majority of studies quoted in the literature have been carried out between the wavelengths 320-380 nm [30-32]. The light that gives rise to the required radiation field can be produced by artificial lamps or by solar irradiation [32].

In a photocatalytic reactor, UV-A (320-380 nm) radiation is provided by fluorescent low-pressure mercury lamps emitting low-intensity UV-A radiation. Medium pressure mercury lamps have also been used, which emit high intensity UV light in the short, medium and long UV spectrums. However, short (UV-C; 200-280 nm) and medium (UV-B; 280-320 nm) UV radiation emitted by the mercury is usually cut off by the photoreactor material, unless it is made of

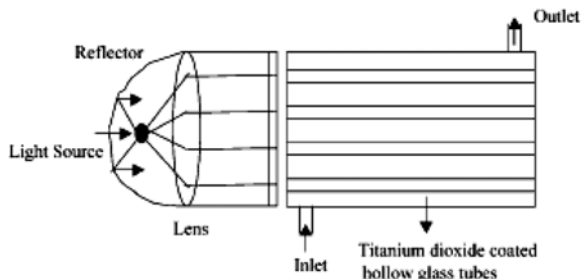
quartz.

Some studies have also reported increased efficiency with UV-C radiation than UV-A for the degradation of certain organic materials [33,34]. Direct photolysis and the higher probability of trapping of electron-hole pairs with shorter wavelength excitation were thought

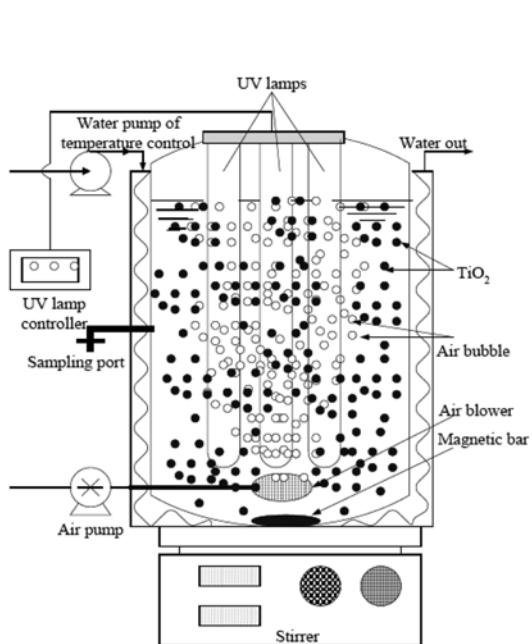
to be the possible reasons for such an effect. It is estimated that only 5% of the incident solar irradiation is of use for the TiO<sub>2</sub> band gap photocatalytic reaction. This significantly limits its practical application. Therefore, modification of TiO<sub>2</sub> photocatalysts to enhance light absorption and photocatalytic activity under visible light irra-



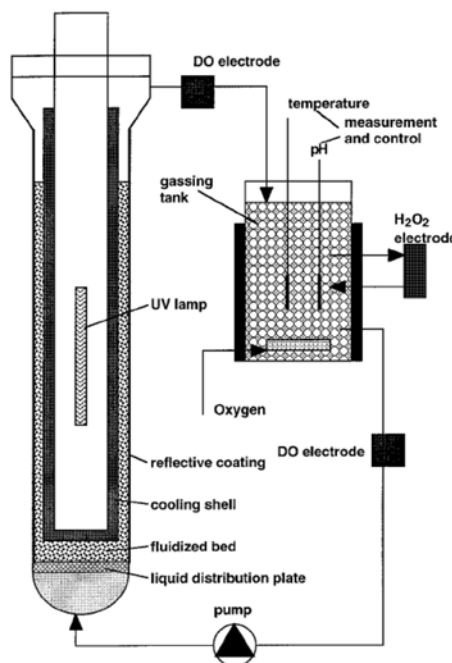
(a) Section of novel tube light reactor [36]



(b) Multiple tube reactor [37]



(c) TiO<sub>2</sub> suspension type reactor [39]



(d) Schematic of fluidised bed photoreactor [40]

Fig. 2. Different types of photocatalytic reactors (a)-(d).

diation is the subject of recent research [35].

#### 4. Photoreactor

The optical path of the light within the reactor governs the choice of photoreactor geometries, which further determines how much radiation is absorbed by the reacting suspension and therefore determines the efficiency of the photocatalytic process. The most usual geometries [16,34,36-38] used for heterogeneous photocatalysis include the following (Fig. 2(a)-(d)):

- Immersion well photoreactor: this is a stirred-tank reactor in which the catalyst is suspended in liquid while the lamp immersed in the suspension [39,41,42].
- Annular photoreactor: two coaxial cylinders surround the lamp placed on the axis.
- Elliptical photoreactor: this consists of a reflecting cylinder of elliptical cross section whose foci are occupied, respectively, by the lamp and the tubular reactor.
- Multi-lamp photoreactor: this set-up consists of a tubular reactor irradiated from the outside by many lamps.
- Film type photoreactor: in this set-up the catalyst particles are deposited on the plane by forming a layer over which the liquid flows as a film. The catalyst is irradiated through the liquid film or through the transparent plane supporting the catalyst.
- Fluidized bed photoreactor [40,43]: This novel photoreactor has a narrow annulus fluidized bed consisting of small TiO<sub>2</sub>-coated quartz sand particles. This configuration meets the requirements of higher surface area-to-volume ratio (which is much lower in fixed-bed configurations), makes better use of light, and shows improvement in mass transfer conditions. It is possible to control and to improve the penetration of light into the fluidized bed by varying its expansion. Na et al. [44] adopted the photocatalytic fluidized bed reactor for the treatment of dye wastewater. Air was supplied into the reactor to keep the TiO<sub>2</sub>-coated hollow ceramic balls in a fluidized state.

#### 5. Solar Reactors

Major design issues for solar photocatalytic reactors are whether to use concentrated or non-concentrated sunlight and whether to use a suspended or supported catalyst.

In light-concentrating systems the solar light is concentrated onto a photocatalytic reactor by a reflecting surface. The main advantage of a concentrating system over a non-concentrating system is it requires smaller reactor volume for the same light-harvest area. Moreover, they can be operated at much higher flow rates, thereby improving mass transfer rates. On the other hand, the lack of reflecting surfaces for the non-concentrating system reduces optical losses. Moreover, this system is known to use more sunlight as it is capable of capturing the diffuse UV light as well as direct solar beams [32]. This allows its operation even under cloudy conditions. However, the non-concentrating system faces certain disadvantages of pressure limitation and the demand for large reactor volumes (as it acts both as a solar collector and photocatalytic reactor) [32].

The operation of the reactor can be a continuous single pass or in a batch mode. A schematic of single-pass and batch modes is given in Fig. 3. A sketch of solar photoreactor is shown in Fig. 4.

In the single pass mode, the reactor area and the flow rates must be carefully taken into account to ensure that the desired destruction of pollutants is achieved in a single-pass. As the UV flux density decreases, the flow rate through the solar reactor must be de-

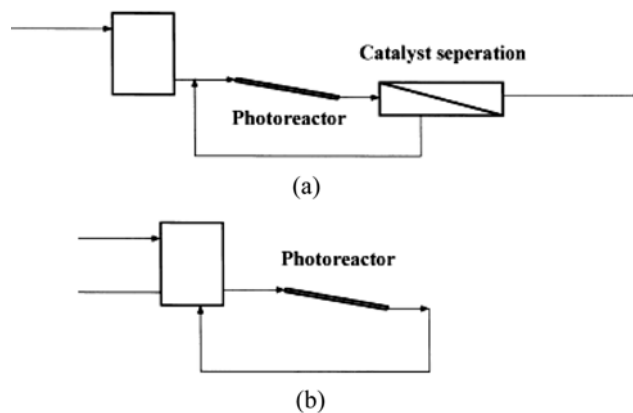


Fig. 3. Schematic representation of two different types of operations of solar photocatalytic reaction (a) single-pass mode (b) batch mode.

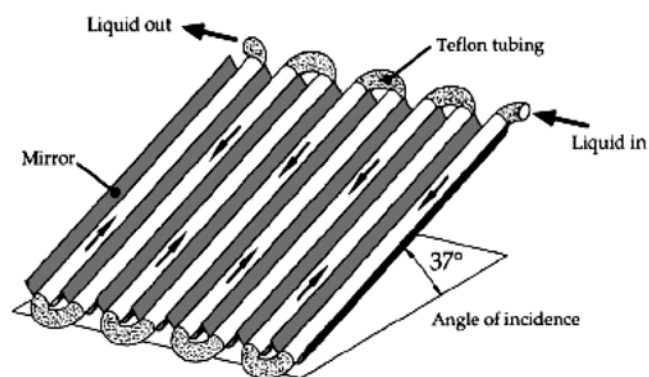


Fig. 4. Schematic representation of solar photoreactor [32].

creased (alternatively, the number of reactors has to be increased) [32]. In the discontinuous batch mode, the wastewater is stored in the tank and continuously recirculated through the solar reactor until the desired final concentration of the pollutant is achieved. Most solar photocatalytic wastewater treatment plants have been operated in the batch mode.

Different kinds of solar reactors have been reported [32];

- Parabolic Trough Reactor (PTRs): It consists of a parabolic shaped light reflecting surface (surface covered with reflective polymer film) with the reaction pipe in its focal line (Fig. 5(a)). TiO<sub>2</sub> is either used as suspension in the tube or bonded onto the surface [32,45].
- Compound Parabolic Collecting Reactor (CPCRs): The shape of the CPCPR reflector consists of two half cylinders of parabolic profile set side by side. The reaction tube is placed in its focal point which is just above the connection of two parabolic profiles (Fig. 5(b)) [32,45].
- Double Skin Sheet Reactor (DSSR): It consists of a non-concentrating double-skin sheet (PLEXIGLAS®) structured box type photoreactor. The suspension containing the polluted water together with the photocatalyst meanders through the channels in the box [32,46,47].
- Thin film fixed bed reactor (TFFBR): It consists of a sloping glass plate coated with photocatalyst. The polluted water flows along the inclined surface forming a very thin film [32,47].

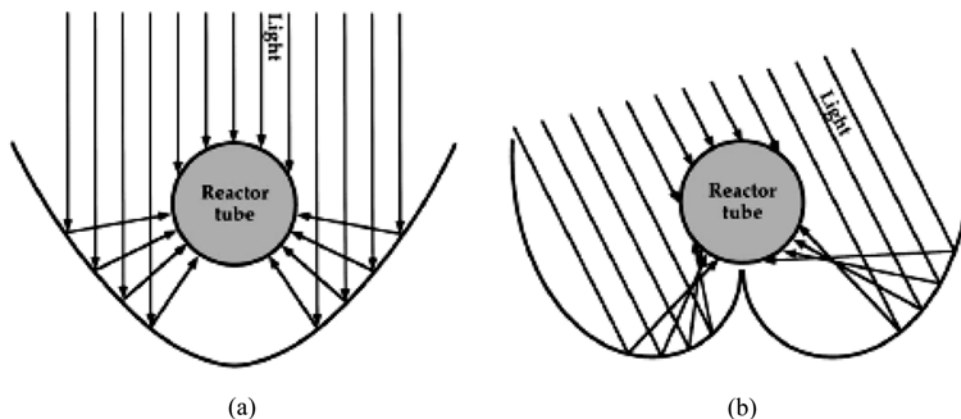


Fig. 5. Geometric profiles of (a) parabolic trough reactor (PTR) and (b) compound parabolic collecting reactor (CPCR) [32].

Careful site treatability studies and establishment of an appropriate pre-treatment are very important prerequisites for successful development of the solar photocatalysis process [48]. It was noted that the solar photocatalytic process will be a suitable technology as the final stage of purification of biologically or physically treated wastewater, and industrial application of this process on a larger scale is in strong demand for cheap photocatalysts with higher activity to be competitive with treatment methods already established on the market [49].

#### 6. Mode of TiO<sub>2</sub> Addition

In photocatalytic degradation using UV/TiO<sub>2</sub>, two modes of TiO<sub>2</sub> application are adopted: (1) TiO<sub>2</sub> immobilized on support materials, e.g., quartz sand, glass, glass wool matrix, ceramic membrane, noble metal etc., and (2) TiO<sub>2</sub> suspended in aqueous medium [41,50-53]. In terms of technical application, immobilized TiO<sub>2</sub> is preferable [31] compared to dispersed TiO<sub>2</sub> because it does not need additional post-treatment for the recovery of catalyst particles after oxidation. However, the problem of scouring or detachment of the deposited catalyst particles was reported in earlier studies with films comprising immobilized powders of TiO<sub>2</sub> [54]. Moreover, during the heating process, which is used for fixing the photocatalyst, a part of the porous structure gets lost through a sintering process. These reduce the area-to-volume ratio of the photocatalyst, which causes ineffective mass transfer. Hence, the efficiency of reactors with immobilized photocatalysts seems to be generally lower than those designs using dispersed TiO<sub>2</sub> particles (slurry) [33,50]. In the case of dispersed TiO<sub>2</sub>, an increase of photocatalytic degradation efficiency by at least a factor of 10 has been reported [50,55] compared to TiO<sub>2</sub> applied in fixed-bed configurations [56].

It is also well known that PAC can be very efficient when it is mixed with TiO<sub>2</sub> in suspension in photocatalytic processes [57,58]. Arana et al. [57] observed that 1) the combination of PAC and TiO<sub>2</sub> results in fast decantability in comparison with that of TiO<sub>2</sub> alone, 2) a TiO<sub>2</sub> particle distribution on the PAC surface yields a homogeneous particle size distribution, and 3) the rate of organic removal by the PAC and TiO<sub>2</sub> was six times higher than that with TiO<sub>2</sub> alone.

#### 7. Photocatalytic Membrane Hybrid System

The use of slurries in photocatalytic wastewater treatment systems requires a post-treatment of separation of catalyst particles. Separation of TiO<sub>2</sub> particles from suspension is usually carried out through physicochemical processes like filtration, centrifugation and

coagulation. There have been some attempts previously in coupling photocatalysis with membrane processes [41,43,59-63].

TiO<sub>2</sub> powders are very fine with an average primary particle size of about 21 nm (Degussa). However, in aqueous media the particles form aggregates within the micron range. This allows the use of porous membrane-like microfiltration for its separation [59]. Molinari et al. [61,62] studied the TiO<sub>2</sub> in suspension in the reactor entrapped by the membrane (Fig. 6) and having the membrane separately from the photoreactor, which was also studied by Xi and Geissan [59] (Fig. 7). Placing the membrane inside the photoreactor could damage the membrane due to the possible membrane oxidation by •OH

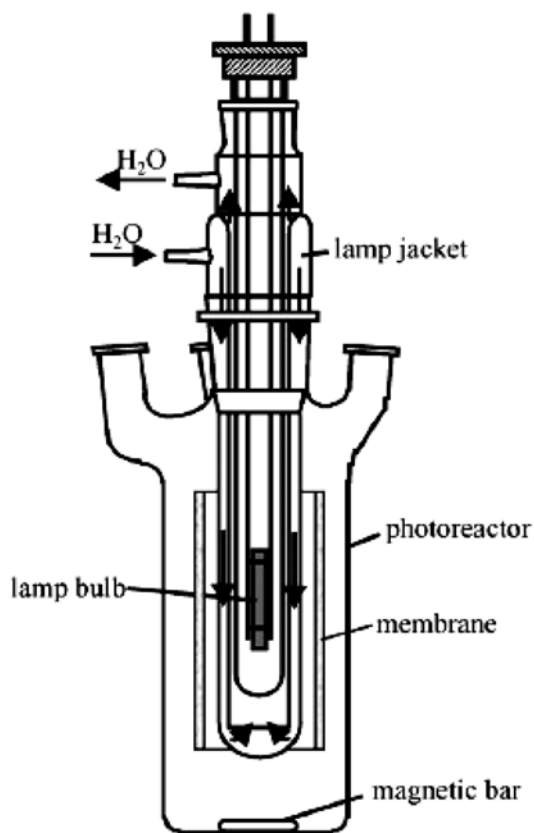


Fig. 6. Batch photoreactor with TiO<sub>2</sub> entrapped by the membrane placed around the bulb of the lamp [61].

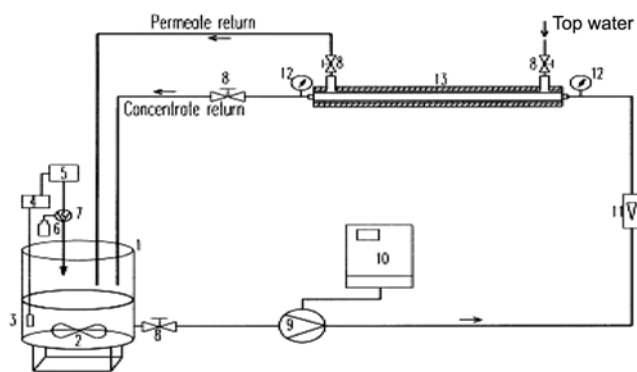


Fig. 7. TiO<sub>2</sub> separation using cross flow microfiltration membrane [59].

- |  |                        |
|--|------------------------|
| 1. Feed vessel                               | 8. Blocking valve      |
| 2. Magnetic stirrer                          | 9. Centrifugal pump    |
| 3. pH electrode                              | 10. Frequency inverter |
| 4. pH meter                                  | 11. Flow meter         |
| 5. pH controller                             | 12. Pressure gauge     |
| 6. Acid (or base) solution                   | 13. Filter module      |
| 7. Peristaltic pump for acid (base) solution |                        |

radicals attack. However, having the UV irradiation lamp outside the reactor would decrease the depth of penetration of UV light because of strong absorptions by TiO<sub>2</sub> and dissolved organic species.

Attempting to separate TiO<sub>2</sub> particles directly from the photocatalytic process could lead to significant membrane fouling, resulting in sharp decline in permeate flux. Moreover, when complete organic degradation is not achieved in the photoreactor, interactions between the two solutes in the system, the residual organic material and the TiO<sub>2</sub> photocatalysts, play a significant role in the formation of dense

cake layers at the membrane surface, leading to a greater membrane fouling and flux decline during membrane operation. The organic-laden TiO<sub>2</sub> particles offered more than four times higher specific cake resistance with a substantially increased compressibility coefficient than TiO<sub>2</sub> particles alone [43].

In order to prevent or lower the membrane fouling, coagulation and sedimentation stages were introduced between photocatalytic oxidation and membrane separation [41]. Submerged hollow fibre microfiltration membrane (PVDF, 0.2 μm) was used as a final step, which obtained reusable quality water. In the separation of very fine TiO<sub>2</sub> particles, solid-liquid separation is influenced by interfacial effects of the aggregates rather than by the size of the primary particles [59]. The change of electrostatic repulsive and van der Waals attractive interactions between particles results in the flocculation of the particles and leads to the formation of flocs and produces a good separation from the liquid. Ferric chloride or iron (II) sulphate was used as the coagulant. Effective TiO<sub>2</sub> removal by coagulation using aluminium chloride as coagulant was earlier reported by Kagaya et al. [64]. A two-step coagulation and sedimentation process followed by submerged hollow fibre microfiltration was found to completely remove TiO<sub>2</sub> from water, and the membrane fouling was significantly reduced, compared to carrying out membrane separation without intermediate coagulation step [41]. A schematic of the two-step coagulation-sedimentation process followed by membrane separation is shown in Fig. 8. The flow chart of the treatment sequence involved as a post-treatment to photocatalytic oxidation for effective separation of TiO<sub>2</sub> photocatalyst is given in Fig. 9. Fig. 10 shows the scanning electron microscope (SEM) images of the particles retained on the membrane after direct filtration after the photocatalytic process and by adopting the two stage coagulation and sedimentation followed by microfiltration membrane hybrid process. Most of the particles were removed by coagulation and sedimentation.

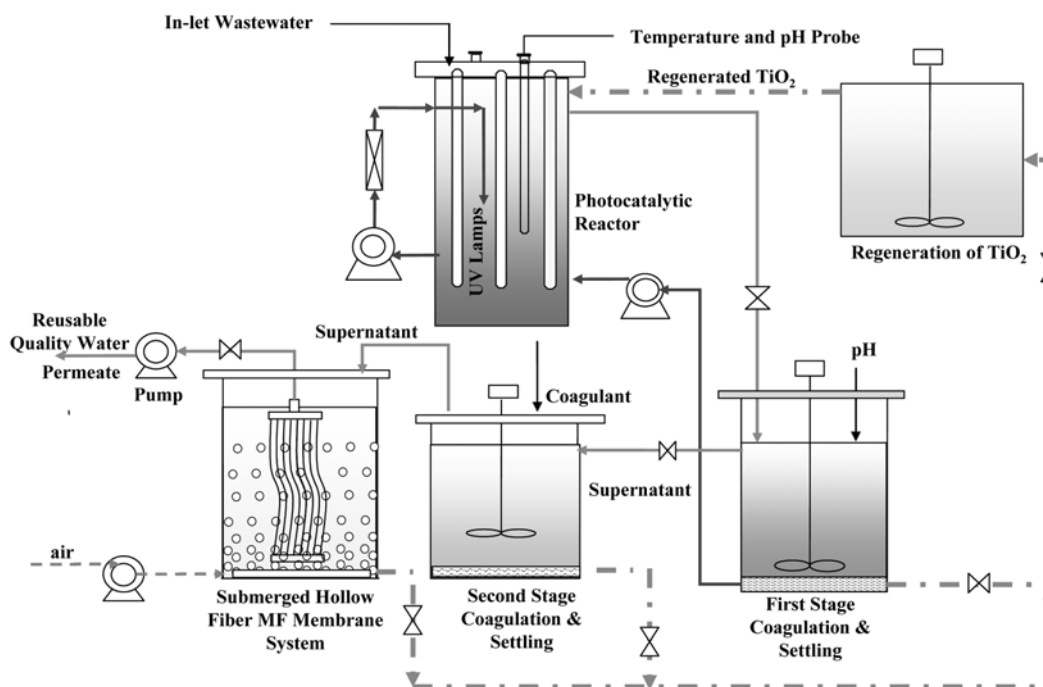
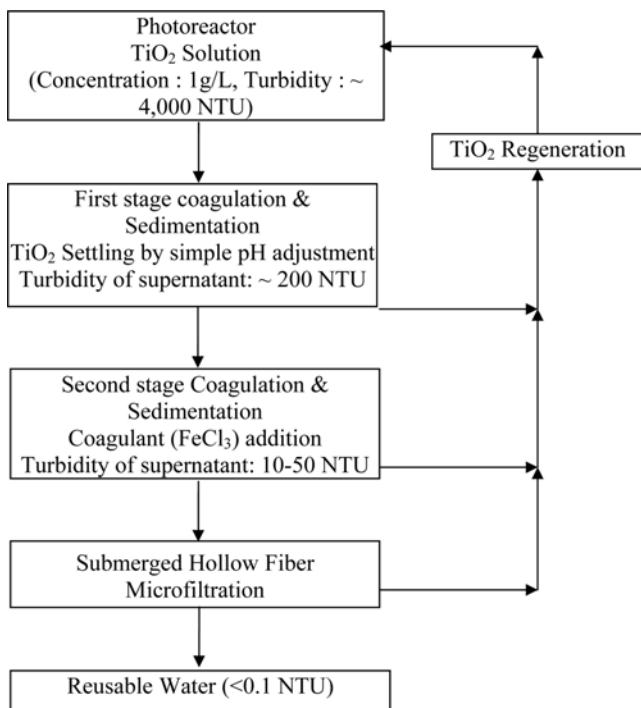


Fig. 8. Schematic of photocatalytic membrane hybrid system.



**Fig. 9. Flow chart of post photocatalytic oxidation treatment for  $\text{TiO}_2$  separation.**

tion and decreased membrane fouling. Complete  $\text{TiO}_2$  separation was achieved, represented by the reduction in turbidity from about 4,000 NTU to less than 0.1 NTU. In a study by Sopajaree et al. [65, 66], with integrated photoreactor-ultrafiltration hollow fibre membrane operation, the  $\text{TiO}_2$  recycled to the photoreactor (10 repeat cycles) noted a systematic degradation in the photocatalyst performance with each repeat cycle. Hence, a regeneration step for the  $\text{TiO}_2$  recovered will regenerate its photocatalyst capacity.

## CONCLUSIONS

A comprehensive review of the UV- $\text{TiO}_2$  photocatalytic oxidation process was carried with an insight into the mechanism involved, catalyst  $\text{TiO}_2$ , irradiation sources, types of reactors, comparison between effective modes of  $\text{TiO}_2$  application as immobilized on surface or as suspension, and photocatalytic hybrid membrane system. The most important and fundamental elements for a successful photocatalytic system are the catalyst, the light source and the reactor configuration.

$\text{TiO}_2$  has greater photocatalytic efficiency than  $\alpha\text{-Fe}_2\text{O}_3$ ,  $\text{ZrO}_2$ ,  $\text{CdS}$ ,  $\text{WO}_3$  and  $\text{SnO}_2$ , and is photochemically more stable in aqueous media. Modification of  $\text{TiO}_2$  photocatalysts to enhance light absorption and photocatalytic activity under visible light irradiation is presently being attempted by the research community. Application of  $\text{TiO}_2$  in a slurry type reactor increases the organic degradation efficiency by at least a factor of 10 when compared to using  $\text{TiO}_2$  immobilized onto support materials. Recovery of  $\text{TiO}_2$  particles by adopting a photocatalytic membrane hybrid system was found to be very efficient and capable of completely removing  $\text{TiO}_2$  from suspension. The influent wastewater turbidity for 1 g/L  $\text{TiO}_2$  was about 4,000 NTU and the final turbidity of the solution after treat-

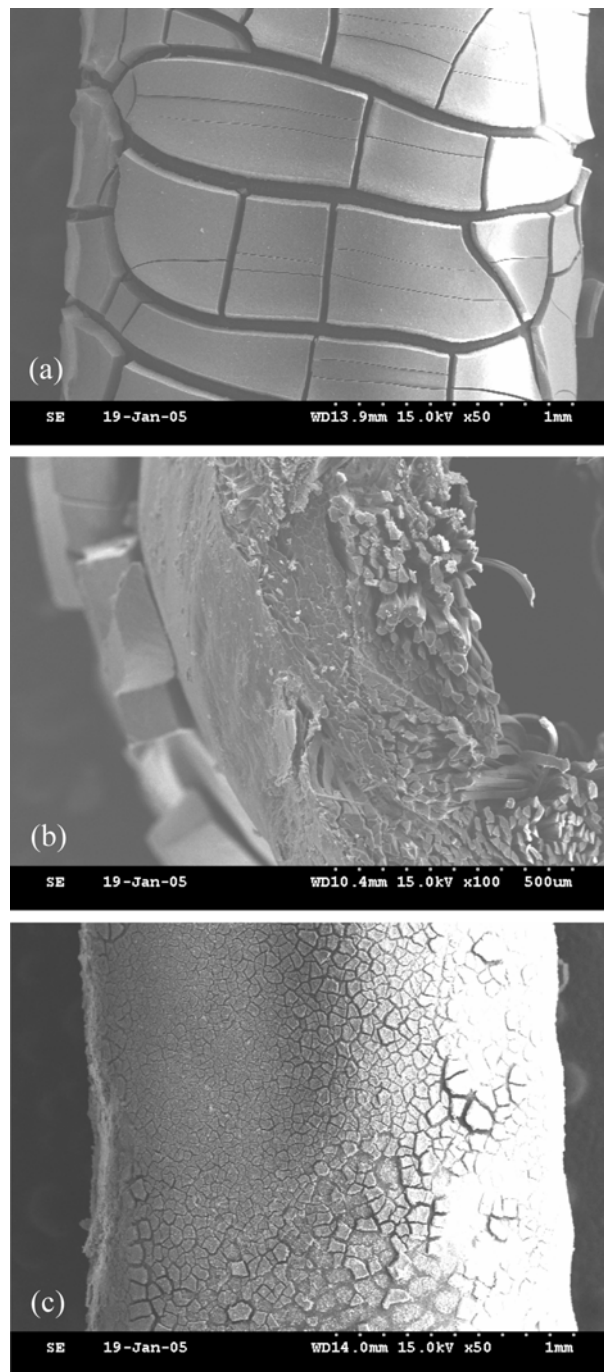


**Fig. 10. SEM images of the membrane used in the separation of  $\text{TiO}_2$  particles in suspension by photocatalytic membrane hybrid system (a) cake deposit on the membrane surface after photocatalytic membrane hybrid system (b) cross section of the membrane showing the thickness of the cake deposit (c) particle deposits on membrane surface after two stage coagulation and sedimentation.**

ment was less than 1 NTU. Adopting a two-stage coagulation and sedimentation stage before the membrane filtration significantly eliminated the particles in suspension, thereby lowering the strain on the membrane. This would lower membrane fouling and prolong the life of the membrane. The recovered  $\text{TiO}_2$  particles can be

reused for the photocatalytic process after regeneration.

The advantages of UV/TiO<sub>2</sub> photocatalysis include operation at low temperature and pressure, low cost and significantly low energy consumption. Application of TiO<sub>2</sub> in suspension instead of immobilizing the TiO<sub>2</sub> on solid carriers has shown an increase in organic degradation efficiencies. However, TiO<sub>2</sub> slurry requires additional separation stages after the photocatalytic process. Moreover, higher TiO<sub>2</sub> concentration in suspension actually decreases the degradation efficiency as the capacity of UV light penetration is significantly decreased due to higher turbidity. An immobilized TiO<sub>2</sub> system eliminates post-treatment stages; however, studies indicate that the degradation performance is reduced due to limiting mass transfer and loss of photocatalytic activity by the fixation procedure.

This technology has the potential for an efficient and sustainable treatment operation with the combination of solar energy as the irradiating light source and effective recovery and regeneration of photocatalyst TiO<sub>2</sub> particles.

#### ACKNOWLEDGMENT

This study was funded by ARC Discovery grant. The first author was with UTS at the time of this study.

#### REFERENCES

1. S. N. Frank and A. J. Bard, *J. Phys. Chem.*, **81**, 1484 (1977).
2. A. L. Pruden and D. F. Ollis, *J. Catal.*, **82**, 404 (1983).
3. C.-Y. Hsiao, C.-L. Lee and D. F. Ollis, *J. Catal.*, **82**, 418 (1983).
4. D. F. Ollis, C. Y. Hsiao, L. Budiman and C. L. Lee, *J. Catal.*, **88**, 89 (1984).
5. D. F. Ollis, *Environ. Sci. & Technol.*, **19**, 480 (1985).
6. S. Sappideen, PhD Dissertation, UNSW (2000).
7. J. W. Tang, Z. G. Zou, J. Yin and J. Ye, *Chem. Phys. Lett.*, **382**, 175 (2003).
8. N. Serpone and E. Pelizzetti, *Photocatalysis: Fundamentals and applications*, John Wiley & Sons, New York (1989).
9. M. Schiavello and A. Sclafani, *Thermodynamics and kinetic aspects in photocatalysis, Photocatalysis: Fundamentals and applications*, John Wiley & Sons, Canada (1989).
10. S. Sakthivel, B. Neppolian, B. Arabindoo, M. Palanichamy and V. Murugesan, *J. Sci. Ind. Res.*, **59**, 556 (2000).
11. K. Okomoto, Y. Yamamoto, H. Tanaka and A. Itaya, *Bull. Chem. Soc. Jpn.*, **58**, 2023 (1985).
12. K. Okomoto, Y. Yamamoto, H. Tanaka and A. Itaya, *Bull. Chem. Soc. Jpn.*, **58**, 2015 (1985).
13. V. Augugliaro, L. Palmisano and A. Sclafani, *Tox. Environ. Chem.*, **16**, 89 (1988).
14. M. Trillas, M. Pujol and X. Domenech, *J. Chem. Tech. Biotechnol.*, **55**, 85 (1992).
15. M. Kaneko and N. Okuru, *Photocatalysis: Science and technology*, Kodansha Ltd, Japan. 356 (2002).
16. P. R. Gogate and A. B. Pandit, *Adv. Environ. Res.*, **8**, 501 (2004).
17. C. H. Wu, *Chemos.*, **57**, 601 (2004).
18. A. P. Rivera, K. Tanaka and T. Hisanaga, *App. Catal. B: Environ.*, **3**, 37 (1993).
19. E. Pelizzetti and C. Minero, *Elect. Acta.*, **38**, 47 (1993).
20. P. H. Chen and C. H. Jeng, *Water. Sup.*, **13**, 29 (1995).
21. X. S. Ye, J. Sha, Z. K. Jiao and L. D. Zhang, *Nanostruct. Mater.*, **8**, 919 (1997).
22. B. Sun and P. G. Smirniotis, *Catal. Today*, **88**, 49 (2003).
23. T. Weng, *Photocatalytic purification and treatment of water and air*, Elsevier Publishers, Amsterdam (1993).
24. J. R. Smyth and D. L. Bish, *Crystal structures and cation sites of the rock-forming minerals*, Allen & Unwin, London (1988).
25. R. I. Bickley, T. Gonzalez-Carreno, J. S. Lees, L. Palmisano and R. J. D. Tilley, *J. Sol. St. Chem.*, **92**, 178 (1991).
26. P. Reeves, R. Ohlhausen, D. Sloan, K. T. Scoggins, C. Clark, B. Hutchinson and D. Green, *Sol. Ene.*, **48**, 413 (1992).
27. R. R. Beska and J. Kiwi, *App. Catal. B: Environ.*, **16**, 19 (1998).
28. S. Yamazaki, S. Matsunaga and K. Hori, *Water Res.*, **35**, 1022 (2001).
29. N. Xu, Z. Shi, Y. Fan, J. Dong, J. Shi and M. Z.-C. Hu, *Ind. Eng. Chem. Res.*, **38**, 373 (1999).
30. O. Legrini, E. Oliveros and A. M. Braun, *Chem Rev.*, **93**, 671 (1993).
31. M. R. Hoffmann, S. T. Martin, W. Choi and D. W. Behnemann, *Chem. Rev.*, **93**, 69 (1995).
32. O. M. Alfano, D. Bahnemann, A. E. Cassano, R. Dillert and R. Goslich, *Catal. Today*, **58**, 199 (2000).
33. R. W. Matthews and S. R. McEvoy, *J. Photochem. Photobiol. A: Chem.*, **64**, 231 (1992).
34. G. L. Puma and P. L. Yue, *Ind. Eng. Chem. Res.*, **38**, 3238 (1999).
35. K. Demeestere, J. Dewulf and B. De Witte, *App. Catal. B: Environ.*, **60**, 93 (2005).
36. A. K. Tod, *Catal.*, **44**, 357 (1998).
37. A. K. Ray and A. A. C. M. Beenackers, *AIChE J.*, **44**, 477. **40**, 73 (1998).
38. C. Tang and V. Chen, *Water Res.*, **38**, 2775 (2004).
39. H. Shon, *Ultrafiltration and nanofiltration hybrid systems in wastewater treatment and reuse*, PhD Dissertation. UTS (2005).
40. A. Haarstrick, O. M. Kut and E. Heinzle, *Environ. Sci. Technol.*, **30**, 817 (1996).
41. R. Thiruvengatchari, T. O. Kwon and I. S. Moon, *Sep. Sci. Technol.*, **40**, 2871 (2005).
42. P. L. Yue, *Water Sci. Technol.*, **35**, 189 (1997).
43. J. C. Lee, M. S. Kim, C. K. Kim, C. H. Chung, S. M. Cho, G. Y. Han, K. J. Yoon and B. W. Kim, *Korean J. Chem. Eng.*, **20**, 862 (2003).
44. Y. S. Na, D. H. Kim, C. H. Lee, S. W. Lee, Y. S. Park, Y. K. Oh, S. H. Park and S. K. Song, *Korean J. Chem. Eng.*, **21**, 430 (2004).
45. C. S. Turchi, J. F. Klausner and E. Marchand, *Field test results for the solar photocatalysis detoxification of fuel-contaminated groundwater*, Chemical Oxidation: Technology for the Nineties, 3<sup>rd</sup> International Symposium (1993).
46. R. Dillerst, S. Vollmer, M. Schober, J. Theurich, D. Bahnemann, H. J. Arntz, K. Pahlmann, J. Wienefeld, T. Schmedding and G. Sager, *Chem. Eng. Technol.*, **22**, 931 (1999).
47. I. Arslan, I. A. Balcioglu and D. W. Bahnemann, *Water Sci. Technol.*, **44**, 171 (2001).
48. D. Y. Goswami, *J. Sol. Ene. Eng.*, **119**, 101 (1997).
49. H. Freudenhammer, D. Bahnemann, L. Bousselmi, S. U. Geissen, A. Ghrabi, F. Saleh, A. Si-Salah, U. Siemon and A. Vogelpohl, *Water Sci. Technol.*, **35**, 149 (1997).
50. C. Guillard, H. Lachheb, A. Houas, M. Ksibi, E. Elaloui and J.-M. Herrmann, *J. Photochem. Photobiol. A: General*, **158**, 27 (2003).
51. M. A. Anderson, S. Tunesi and Q. Xu, US patent 5035784 (1991).
52. G. A. Cooper, US Patent 4888101 (1989).

53. J. Oonada, JP Patent 06071256, (1994).
54. M. Bideau, B. Claudel, C. Dubien, L. Faure and H. Karzouan, *J. Photochem. Photobiol. A. Chem.*, **91**, 137 (1995).
55. A. M. Braun, *In photochemical conversion and storage of solar energy*, 8<sup>th</sup> International Conference on Photochemical Conversion and Storage of Solar Energy, Palermo, Italy (1990).
56. K. Hofstadler, R. Bauer, S. Novalic and G. Heisler, *Environ. Sci. Technol.*, **28**, 670 (1994).
57. J. Arana, J. A. H. Melian, J. M. D. Rodriguez, O. G. Diaz, A. Viera, J. P. Pena, P. M. M. Sosa and V. E. Jimenez, *Catal. Today*, **76**, 279 (2002).
58. J. Arana, J. M. Dona-Rodriguez, R. E. Tello, I. Garriga, C. Cabo, O. Gonzalez-Diaz, J. A. Herrera-Melian, J. Perez-Pena, G. Colon and J. A. Navio, *App. Catal. B: Environ.*, **44**, 161 (2003).
59. W. Xi and S.-U. Geissen, *Wat. Res.*, **35**, 1256 (2001).
60. R. Molinari, M. Mungari, E. Drioli, A. Di Paola, V. Loddo, L. Palmisano and M. Schiavello, *Catal. Today*, **55**, 71 (2000).
61. R. Molinari, L. Palmisano, E. Drioli and M. Schiavello, *J. Mem. Sci.*, **206**, 399 (2002).
62. R. Molinari, F. Pirillo, M. Falco, V. Loddo and L. Palmisano, *Chem. Eng. Pro.*, **43**, 1103 (2004).
63. R. Thiruvengkatachari, T. O. Kwon and I. S. Moon, *Korean J. Chem. Eng.*, **22**, 938 (2005).
64. S. Kagaya, K. Shimizu, R. Arai and K. Hasegawa, *Wat. Res.*, **33**, 1753 (1999).
65. K. Sopajaree, S. A. Qasim, S. Basak and K. Rajeshwar, *J. Appl. Electrochem.*, **29**, 533 (1999).
66. K. Sopajaree, S. A. Qasim, S. Basak and K. Rajeshwar, *J. Appl. Electrochem.*, **29**, 1111 (1999).